WEIGHT OPTIMIZATION FOR MULTIPLE IMAGE INTEGRATION

Ryo Matsuoka, Tomohiro Yamauchi, Tatsuya Baba, Masahiro Okuda

Univ. of Kitakyushu, Faculty of Environmental Engineering, JAPAN

ABSTRACT

We propose a denoising technique using multiple image integration. When acquiring a dark scene, the detail of the dark area is often deteriorated by sensor noise. A simple image integration inherently has the capability of reducing random noises. In this paper we develop the denoising performance of the multiple image integration by optimizing weight maps. We determine the optimal weight by solving a convex optimization problem. Through some experimental results, we show the weight optimization significantly improves the denoising performance.

***Index Terms*—** Image Integration, Denoising, Convex Optimization, High Dynamic Range Images

1. INTRODUCTION

It is a challenging problem to take a sharp photograph without any noise under a low lighting condition. In a long exposure setting, an image is blurred due to object motion and camera shake, while short exposure photography in shadows often requires high ISO sensitivity, which results in noisy images. Many methods have been proposed for denosing and deblurring images [1]-[6]. Image integration is one of the simplest solutions for the denoising problem. Taking the mean of well-aligned multiple images with short exposures can reduce the random noises [3].

In the last decade, demand for high dynamic range (HDR) imaging has been increasing [7]. In general, the HDR image is generated by combining some photographs taken with multiple exposure settings [7]-[11]. To get a high dynamic range, several photographs with short to long exposures are integrated. When taking photographs with a hand held camera in a dark lighting condition, a high ISO setting is required to restore the dark area without blurring artifacts, which yields noisy images. The dynamic range of a sensor is usually defined by the maximum achievable signal intensity divided by the maximum level of the camera noise, and thus the sensor noise brings down the dynamic range.

In [6], a weight function is designed to reduce sensor noises and quantization noises, but it is not optimal in any sense. Recently, a weight optimization method is proposed in [12] for the image integration. The main purpose of the method is image-stitching, and they do not consider the multiple image denoising.

In this paper, we propose a method for the multiple image integration. The main contribution of the proposed method is that we find the optimal weight by using a convex optimization technique. We show that the weight optimization significantly improves the capability of denoising compared to conventional approaches.

In the following section, we explain the multiple image integration procedure including the HDR acquisition. In Section 3, we introduce a method for the weight optimization. The problem is formulated as a convex optimization problem, and it is solved by the primal-dual splitting approach [13]. In Section 4, we simulate our method with some images with actual sensor noise, and then we compare results with conventional denoising approaches, and quantitatively show the validity of the method.

2. MULTIPLE IMAGE INTEGRATION

Let $\mathbf{l}_k \in \mathbb{R}^N$ $(k = 1, 2, \cdots, K)$ be vectors representing noisy observed images with N pixels. The multiple image integration can be expressed by the linear combination of the K weighted images $\mathbf{L}_k\mathbf{w}_k$, $(k = 1, 2, \cdots, K)$:

$$\mathbf{h} = \sum_{k=1}^{K} \mathbf{L}_k \mathbf{w}_k \tag{1}$$

where $\mathbf{L}_k \in \mathbb{R}^{N\times N}$ is a $(N \times N)$ diagonal matrix $\mathbf{L}_k = diag\{\mathbf{l}_k\}$, where $\mathbf{w}_k$ $(\in \mathbb{R}^N)$ is a set of weight maps. To preserve the energy of the image, the weight maps are normalized to $\sum_{k=1}^{K} \mathbf{w}_k = \mathbf{1}$, where $\mathbf{1} \in \mathbb{R}^N$ is the vector of all ones.

In a case of the multiple exposure integration, to accurately linearize the images, we need to compensate for the nonlinearity by estimating the inverse g^{-1} of an in-camera intensity transform [7]. Here we call the transform a "camera response curve" denoted by g that gives the relationship $\hat{\mathbf{l}}_k = g(\bar{\mathbf{l}}_k)$, where $\hat{\mathbf{l}}_k$, $\bar{\mathbf{l}}_k \in \mathbb{R}^N$ are an observed image and a sensor output, respectively. If one uses raw images, and an image sensor has a linear sensitivity characteristic, this photometric calibration can be skipped. Among existing methods for the calibration problem, we adopt Mitsunaga et al.'s method [10] to find g^{-1}, in which the curve is approximated

Thanks to JSPS and KDDI foundation for funding.

by a low order polynomial using multiple images and exposure values. Once the curve is estimated, the images are linearized by $\mathbf{l}_k = g^{-1}(\hat{\mathbf{l}}_k)/t_k$, where t_k is an exposure time of the k-th image. In our method, the multiple exposure images are taken by varying the exposure time of a camera with other settings fixed. Then the images are merged by (1) to create the HDR image.

3. PROPOSED METHOD

In our framework, we need to find the denoised image $\mathbf{h}$ and the weight $\mathbf{w}_k$ with $\mathbf{l}_k$ given. Finding the optimal values for the two variables simultaneously inherently leads to ill-posed and non-convex optimization. Thus we first use the conventional weight in [8] as an initial guess and then construct $\mathbf{h}$ using the method in Sec. 3.1. With the obtained image, we optimize the weight as is explained in Sec. 3.2. Finally we again apply the method in Sec. 3.1 with the optimal weights to obtain a final result.

3.1. TV Denoising

To find $\mathbf{h}$, we adopt the conventional Total Variation denoising method [14]. Given the weight $\boldsymbol{w}_k$, the problem is defined as

$$\min_{\mathbf{h}} \ \| \sum_{k=1}^{K} \mathbf{L}_k \mathbf{w}_k - \mathbf{h} \|_2^2 + \gamma \, \| \mathbf{h} \|_{TV} \tag{2}$$

where $\|\cdot\|_{TV}$ is the anisotropic Total Variation regularization term. This minimization problem can be solved by a convex optimization method. In the optimization procedure, we iteratively perform the two steps, solving a linear equation and a shrinkage operation. Using the diagonalization by FFT and a soft-thresholding function, one can obtain the solution quickly (for detail, see [14]).

3.2. Weight Optimization

The optimization for the weight $\mathbf{w}_k$ is fulfilled by

$$\begin{aligned} &\min_{\mathbf{w}} \ \|\bar{\mathbf{p}}_w - \mathbf{h}\|_2^2 + \alpha \, \|\mathbf{D}\bar{\mathbf{p}}_w\|_1 \\ &\quad \text{s.t.} \ \sum_{k=1}^{K} \mathbf{w}_k = \mathbf{1}, \ \text{ and } \quad \mathbf{w}_k \in S \ (k = 1, 2, \cdots, K) \end{aligned} \tag{3}$$

where $\bar{\mathbf{p}}_w = \sum_{k=1}^{K} \mathbf{L}_k \mathbf{w}_k$, $\mathbf{D} \in \mathbb{R}^{N \times N}$ is a convolution matrix representing a derivative operation, and

$$S = \{\mathbf{x} \in \mathbb{R}^N \mid \ x_i \in [0, 1] \ \ (i = 1, 2, \cdots, N)\}.$$

Using the following relationship

$$\bar{\mathbf{p}}_w = \sum_{k=1}^{K} \mathbf{L}_k \mathbf{w}_k = \sum_{k=1}^{K-1} (\mathbf{L}_k - \mathbf{L}_K) \, \mathbf{w}_k + \mathbf{l}_K \tag{4}$$

and introducing the two matrices, $\mathbf{P} \in \mathbb{R}^{N \times N(K-1)}$ and $\mathbf{w} \in \mathbb{R}^{N(K-1)}$ as

$$\begin{aligned} \mathbf{P} &= [(\mathbf{L}_1 - \mathbf{L}_K) \ \ (\mathbf{L}_2 - \mathbf{L}_K) \ \ \cdots \ \ (\mathbf{L}_{K-1} - \mathbf{L}_K)] \\ \mathbf{w} &= \left[\mathbf{w}_1^T \ \mathbf{w}_2^T \ \cdots \ \mathbf{w}_{K-1}^T\right]^T, \end{aligned}$$

then Eq.(3) is rewritten as an unconstrained problem:

$$\begin{aligned} \min_{\mathbf{w}} \ &\|\mathbf{P}\mathbf{w} + (\mathbf{l}_K - \mathbf{h})\|_2^2 + \alpha \, \|\mathbf{D}(\mathbf{P}\mathbf{w} + \mathbf{l}_K)\|_1 \\ &+ \iota_S(\mathbf{C}\mathbf{w}) + \sum_{k=1}^{K-1} \iota_S(\mathbf{w}_k) \end{aligned} \tag{5}$$

where ι_S denotes the indicator function,

$$\iota_S(\mathbf{v}) = \begin{cases} 0, & \text{if } \mathbf{v} \in S \\ +\infty, & \text{if } \mathbf{v} \notin S, \end{cases} \tag{6}$$

and $\mathbf{C} \in \mathbb{R}^{N \times N(K-1)}$ is a $\{N \times N(K-1)\}$-matrix composed of the $K - 1$ identity matrices

$$\mathbf{C} = \underbrace{[\mathbf{I}_N \ \mathbf{I}_N \ \cdots \ \mathbf{I}_N]}_{K-1}.$$

The third term of (5) guarantees the solution satisfies $\sum_{k=1}^{K} \mathbf{w}_k = \mathbf{1}$ by taking $\mathbf{w}_K = 1 - \sum_{k=1}^{K-1} \mathbf{w}_k$, and the forth term forces $\mathbf{w}_k$ to be in the range $[0, \ 1]$.

The cost function (5) is convex and thus can be solved by the primal-dual splitting approach [13]. The primal-dual algorithm solves the minimization problem of the form

$$\min_{x} F(\mathbf{x}) + G(\mathbf{x}) + H(\mathbf{L}\mathbf{x}), \tag{7}$$

where F, G, H are proper, lower semicontinuous, convex functions in a real Hilbert space, and F is differentiable, and ∇F is β-Lipschitz continuous. L is a bounded linear operator. For the primal-dual algorithm to be applicable to our problem, we set

$$\begin{aligned} F(\mathbf{x}) &= \frac{\alpha}{2} \|\mathbf{P}\mathbf{x} + (\mathbf{l}_K - \mathbf{h})\|_2^2 \\ G(\mathbf{x}) &= 0 \\ \mathbf{L} &= \underbrace{\begin{bmatrix} & \mathbf{DP} & & \\ \hdashline & \mathbf{C} & & \\ \hdashline \mathbf{I}_N & 0 & \cdots & 0 \\ 0 & \mathbf{I}_N & \cdots & 0 \\ & \cdots & & \\ 0 & 0 & \cdots & \mathbf{I}_N \end{bmatrix}}_{K-1} (\in \mathbb{R}^{(N(K+1) \times N(K-1)}) \end{aligned}$$

$$H(\mathbf{u}) = \alpha \, \|\mathbf{x}_a + \mathbf{l}_d\|_1 + \iota_S(\mathbf{x}_b) + \sum_{k=1}^{K-1} \iota_S(\mathbf{x}_{ck})$$

where $\mathbf{l}_d = \mathbf{D}\mathbf{l}_K$ and
$\mathbf{u} = [\mathbf{x}_a^T \ \mathbf{x}_b^T \ \mathbf{x}_{c1}^T \ \mathbf{x}_{c2}^T, \cdots, \mathbf{x}_{c(K-1)}^T]^T, \ \ (\mathbf{x}_* \in \mathbb{R}^N).$

Then, the primal-dual splitting algorithm iteratively finds the two proximal operators[1]

$$
\begin{aligned}
&1.\ \mathbf{x}_{n+1} := \mathrm{prox}_{\gamma_1 G}\left(\mathbf{x}_n - \gamma_1 \nabla F(\mathbf{x}_n) - \gamma_1 \mathbf{L}^* \mathbf{y}_n\right) \\
&2.\ \mathbf{y}_{n+1} := \mathrm{prox}_{\gamma_2 H^*}\left(\mathbf{y}_n - \gamma_2 \mathbf{L}(2\mathbf{x}_{n+1} - \mathbf{x}_n)\right),
\end{aligned} \tag{8}
$$

where ∇F is the gradient of F and L^* is the adjoint of L. The sequence $(\mathbf{x}_n)_{n\in\mathbb{N}}$ weekly converges to the solution of (7) (see [13] for detail). The proximal operators in (8) are given by

$$
\begin{aligned}
&\mathrm{prox}_{\gamma_1 G}(\mathbf{x}) = \mathbf{x}. \\
&\mathrm{prox}_{\gamma_2 H^*}(\mathbf{u}) = \mathbf{u} - \gamma_2 \mathrm{prox}_{H/\gamma_2}\left(\frac{\mathbf{u}}{\gamma_2}\right),
\end{aligned} \tag{9}
$$

where

$$
\begin{aligned}
&\mathrm{prox}_{H/\gamma_2}(\mathbf{u}) = \\
&\quad [P_a(\mathbf{x}_a)^T\ P_b(\mathbf{x}_a)^T\ bP_b(\mathbf{y}_{c1})^T\ ,\cdots, P_b(\mathbf{y}_{c(K-1)})^T]^T.
\end{aligned}
$$

$P_a : \mathbb{R}^N \to \mathbb{R}^N$ is the soft-thresholding operator

$$
P_a(x_i) = \begin{cases} x_i - \alpha/\gamma_2 & \text{if } x_i - \alpha/\gamma_2 > -l_{d,i} \\ x_i + \alpha/\gamma_2 & \text{if } x_i + \alpha/\gamma_2 < -l_{d,i} \\ -l_{d,i} & \text{otherwise} \end{cases}
$$

where $l_{d,i}$ is the i-th element of $\mathbf{l}_d$, and $P_n : \mathbb{R}^N \to \mathbb{R}^N$ is given by

$$
P_n(x_i) = \begin{cases} 0 & \text{if } x_i < 0 \\ x_i & \text{if } 0 \le x_i \le 1 \\ 1 & \text{if } x_i > 1. \end{cases} \tag{10}
$$

From the above discussion, our algorithm can be stated as follows:

1. Set $l = 0$, and $\mathbf{l}_k, \mathbf{w}^{(0)}$ are given.
2. Solve (2) for $\mathbf{w} = \mathbf{w}^{(0)}$.
3. Set $n = 0, \mathbf{x}^{(n)} = \mathbf{w}^{(n)}, \mathbf{y}^{(n)} = \mathbf{L}\mathbf{x}$.
4. $\mathbf{x}^{(n+1)} = \mathrm{prox}_{\gamma_1 G}\left(\mathbf{x}^{(n)} - \gamma_1 \nabla F(\mathbf{x}^{(n)}) - \gamma_1 \mathbf{L}^* \mathbf{y}^{(n)}\right)$
5. $\mathbf{y}^{(n+1)} = \mathrm{prox}_{\gamma_2 H^*}\left(\mathbf{y}^{(n)} - \gamma_2 \mathbf{L}(2\mathbf{x}^{(n+1)} - \mathbf{x}^{(n)})\right)$
6. If the criterion is not satisfied, increment n by 1 and then go to 4.
7. Set $\mathbf{w} = \mathbf{x}^{(n+1)}$ and solve (2).

4. EXPERIMENTAL RESULTS

In the first experiment, we use sets of three images with different exposures, all of which are taken with ISO 100 sensitivity and have little noise. These shots are obtained by changing shutter speed, while the aperture is fixed, and use them as ground truth for our algorithm. We add white Gaussian noise to the images for the inputs. As conventional methods, we adopt the simple weight map in [8] and TV denoising in 3.1, which is essentially same as [14].

The quantitative comparison is listed in Table 1, in which we compare the proposed method with the weight of the hat function (Hat) in [8], and the TV denoising, , which is essentially same as [14], with the hat function (HatW+TV). Note that only the difference between HatW+TV and our method is the weights, and same parameters are used in the TV denosing. For quality metrics, we use SNR[2] of the obtained HDR image and the nonlinear PSNR. The nonlinear PSNR is calculated by applying Reinhard et al.'s tone-mapping [7] to the HDR output to yield its low dynamic range version and then finding its PSNR. Since the HDR image has high dynamic range, noises in its bright regions are overestimated by SNR even though it is less perceivable than noises in shadows. The nonlinear PSNR may be more suitable metric to evaluate HDR images considering the Human Visual System. The image (a)-(c) in the list are shown in Fig. 1(a)-(c). One can see from the results that the weight optimization improves the image quality significantly (see the parts circled in red).

In the second experiment, we take photographs with ISO 1600 to obtain inputs with actual sensor noises, and then apply the methods to them. Fig. (d)-(e) illustrates the results for images with actual sensor noises, which are taken with ISO 1600. We average fifteen photographs and the mean image is set as the ground truth. One can see from the figure that the conventional method (HatW+TV) sometimes overly smooth edges, and lack sufficient denoising especially for bright regions, while our method outperforms it.

The conventional weights such as the hat function play a role of eliminating saturated pixels, while our method does not consider the pixel saturation. In our method, however, by virtue of the first term of (3) the pixel saturation seldom occurs unless the input $\mathbf{h}$ has saturation.

Table 1. SNR and Nonlinear PSNR (NSN), Hat: Hat function, OptW: our optimal weight, HatW+TV: TV denosing with Hat function, and Our method

	Hat		Hat+TV		Our method	
Image	SNR	NSNR	SNR	NSNR	SNR	NSNR
(a)	15.3	23.8	17.4	24.4	**19.3**	**26.4**
(b)	15.4	27.0	19.2	28.2	**20.8**	**32.2**
(c)	14.4	24.6	17.1	26.3	**18.8**	**29.6**

5. CONCLUSION

We introduce a method for the weight optimization. When combining multiple images to obtain the HDR image, noise can be significantly reduced by the optimal weight and the TV denoising technique. We have shown the validity of our method through the numerical simulation for the images with AWGN and actual sensor noises.

[1]The proximal operator for γ and $F(y)$ is defined as

$$
\mathrm{prox}_{\gamma F}(\mathbf{x}) = \arg\min_{y} \|\mathbf{x} - \mathbf{y}\|/2 + \gamma F(\mathbf{y})
$$

[2]Since the HDR image does not have a peak value, PSNR is not used for the comparison

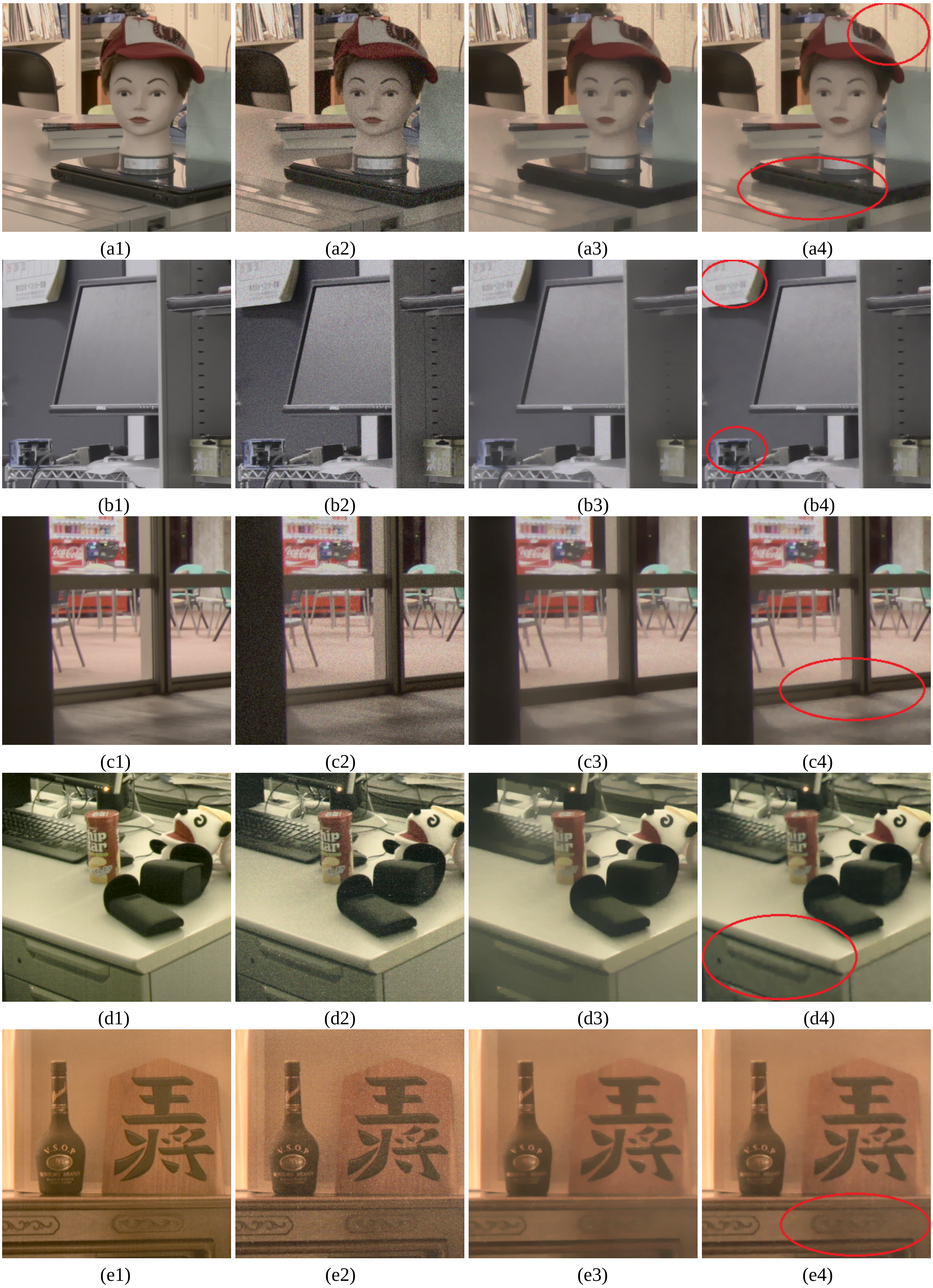

Fig. 1. Results:(from left to right) Ground truth, Simple hat function (Hat), hat function plus TV (Hat+TV), and Our method. (a)-(c): images with AWGN, (d)-(e): images with actual sensor noise

6. REFERENCES

[1] G. Petschnigg, R. Szeliski, M. Agrawala, M. Dohen, H. Hoppe, and K. Toyama, ”Digital photography with flash and no-flash image paris,” in ACM Trans. on Graphics(SIGGRAPH), vol. 23, pp.664-672, 2004.

[2] K. Shirai, M. Ikehara, M. Okamoto, ”Noiseless no-flash photo creation by color transform of flash image,” Image Processing (ICIP), 2011 18th IEEE International Conference on, pp.3437-3440, 11-14 Sept. 2011.

[3] T.Buades, Y. Lou, J.M. Morel and Z. Tang, ”A note on multi-image denoising,” International workshop on Local and Non-local Approximation in Image Processing, pp.1-15, Aug. 2009.

[4] K. Dabov, A. Foi, and K. Egiazarian, ”Image restoration by sparse 3D transform-domain collaborative filtering,” Proc. SPIE Electronic Imaging ’08, no. 6812-07, January. 2008.

[5] Whyte, O., Sivic, J., Zisserman, A., and Ponce, J., ”Non-uniform deblurring for shaken images,” IEEE Conference on Computer Vision and Pattern Recognition (CVPR), pp. 491 - 498, Jun. 2010

[6] Ryo Matsuoka, Masahiro Okuda, ”Multiple Exposure Integration with Image Denoising”, APSIPA Annual Summit & Conference, PS.3-IVM.7, Dec. 2012.

[7] E. Reinhard, S.Pattanaik, G. Ward and P. Debevec, ”High Dynamic Range Imaging: Acquisition, Display, and Image-Based Lighting (Morgan Kaufmann Series in Computer Graphics and Geometric Modeling),” *Morgan Kaufmann Publisher 2005*.

[8] P.E. Debevec and J. Malik, ”Recovering High Dynamic Range Radiance Maps from Photographs,” Proceedings of SIGGRAPH 97, Computer Graphics Proceedings, pp.369-378, 1997.

[9] S. Mann and R. Picard, ”On being ’undigital’ with digital cameras: Extending dynamic range by combining differently exposed pictures,” In Proceedings of IS&T 46th annual conference (May 1995), pp. 422–428. 1995.

[10] T. Mitsunaga, and S. K. Nayer, ”Radiometric Self Calibration, ” IEEE Conference on Computer Vision and Pattern Recognition (CVPR), Vol.1, pp.374-380, Jun, 1999.

[11] Takao Jinno, Masahiro Okuda, ”Multiple Exposure Fusion for High Dynamic Range Image Acquisition,” Image Processing, IEEE Transactions on , vol.21, no.1, pp.358-365, Jan. 2012.

[12] Wei Wang and Michael K. Ng, ”A Variation Method for Multiple-Image Blending,” IEEE Transactions on Image Processing, Vol.21, No.4, pp.1809-1822, April 2012.

[13] L. Condat, “ A primal-dual splitting method for convex optimization involving Lipschitzian, proximable and linear composite terms, ” J. Optimization Theory and Applications, to appear in 2013.

[14] WANG, Y., YANG, J., YIN, W., AND ZHANG, Y. ”A New Alternating Minimization Algorithm for Total Variation Image Reconstruction,” SIAM J. Imaging Sciences 1, 3, 248-272, 2008.

[15] D.Donoho, ”De-noising by soft-thresholding,” Information Theory, IEEE Transactions on , vol.41, no.3, pp.613-627, May 1995.